Dynamic NMR Studies on Hydride and Carbonyl Fluxionality in Triosmium–Platinum Cluster Compounds. X-ray Crystal Structure of $[Os_3Pt(\mu\text{-}H)_3(CO)_{10}(PCy_3)]^+BF_4^-$

Paul Ewing, Louis J. Farrugia,* and David S. Rycroft

Department of Chemistry, University of Glasgow, Glasgow, G12 8QQ, Scotland, U.K

Received September 23, 1987

Variable-temperature ^{13}C NMR studies on $Os_3Pt(\mu\text{-}H)_2(CO)_{10}(PCy_3)$ (1) show three distinct carbonyl exchange processes. The lowest energy process ($\Delta G^{\ddagger}_{233}$ = 49.7 (5) kJ mol^{-1}) involves localized scrambling in two $Os(CO)_3$ groups, while a second process permutes all nine Os-bound CO ligands. A proposed mechanism involving rotation of the PtL_2 fragment, coupled with facial hydride migration, accounts for both this latter process and the simultaneous mutual exchange of the hydride ligands (for which $\Delta G^{\ddagger}_{295}$ = 63.1 (5) kJ mol^{-1}, $\Delta H^{\ddagger}$ = 55 (1) kJ mol^{-1}, $\Delta S^{\ddagger}$ = −27 (3) J mol^{-1} K^{-1}). Above 333 K a final mechanism results in total CO scrambling. Protonation of 1 with HBF_4 affords the trihydrido salt $[Os_3Pt(\mu\text{-}H)_3(CO)_{10}(PCy_3)]^+BF_4^-$ (2) in high yield. Crystal data for 2: monoclinic, space group *Pn*, a = 9.925 (2) Å, b = 11.747 (3) Å, c = 16.186 (4) Å, β = 89.75 (2)°, V = 1887.1 (8) Å^3, Z = 2, final R (R_w) values of 0.032 (0.034) for 4087 independent observed data, $I \geq 3\sigma(I)$. 2 has a tetrahedral framework with the hydrido ligands bridging the Pt–Os(3) edge (2.845 (1) Å) and the Os(1)–Os(3) and Os(1)–Os(2) edges (2.891 (1) and 2.747 (1) Å, respectively), with the other metal–metal edges Pt–Os(1) = 2.812 (1), Pt–Os(2) = 2.819 (1), and Os(2)–Os(3) = 2.790 (1) Å. The two $Os(\mu\text{-}H)Os$ hydrides, unambiguously assigned by using NOE difference spectra, are involved in mutual exchange ($\Delta G^{\ddagger}_{293}$ = 62.7 (5) kJ mol^{-1}). The lower energy carbonyl exchange process, observed in magnetization transfer studies using DANTE, is compatible with the hydride fluxionality, and a higher energy carbonyl exchange is consistent with rotation of the $PtH(CO)(PR_3)$ moiety about the Os_3 triangle. The butterfly adducts $Os_3Pt(\mu\text{-}H)_2(CO)_{10}(PCy_3)(L)$ (3, L = CO; 4, L = PCy_3) show strikingly different fluxional behavior. A highly unusual and very low-energy six-site Pt–Os carbonyl exchange, involving a proposed closo transition state, is observed for 3. In contrast magnetization transfer and ^{13}C 2D exchange correlation NOESY studies on complex 4 show only high-energy CO exchange between Pt and Os and suggest a novel "flipping" of the butterfly framework through a planar transition state. In both compounds the hydrides are nonfluxional at ambient temperature. $^1J(^{187}Os\text{–}^{13}C)$ coupling constants in the range 98–117 Hz are reported for complexes 1–3.

Introduction

The 58-electron triosmium–platinum complex $Os_3Pt(\mu\text{-}H)_2(CO)_{10}(PCy_3)$ (1) (Cy = c-C_6H_{11}) has been shown to possess an essentially regular tetrahedral metal core.[1] Simple application of various polyhedral electron counting procedures[2] thereby suggests that 1 is electronically unsaturated, although it should be noted that platinum-containing cluster complexes usually do not conform to these rules and have fewer valence electrons.[3] Nevertheless, an EHMO study by Hoffmann and Schilling,[4] using the model complex $[Fe_3Pt(CO)_{10}(PH_3)]^{2-}$, indicated a low-lying LUMO. In accordance with this proposed unsaturation, complex 1 is found to be highly reactive toward two-electron donors, L, yielding the 60-electron adducts $Os_3Pt(\mu\text{-}H)_2(CO)_{10}(PR_3)(L)$.[5,6] X-ray studies have shown that these adducts can either have a tetrahedral metal skeleton (L = $(\mu\text{-}H)_2$, R = Cy[5]; L = $(\mu\text{-}CH_2)$, R = Cy[5]) or adopt a butterfly configuration (L = CO, R = Cy[5]; L = PPh_3, R = Ph[6]).

Interestingly the EHMO study[4] also indicated a low barrier to rotation of the PtL_2 moiety about the $M_3(CO)_9$ framework, although the presence of the hydrido ligands in 1 was expected to raise this energy. These hydrido ligands occupy chemically distinct sites, one bridging a Pt–Os vector and the other an Os–Os bond,[1] and variable-temperature ^1H NMR studies revealed a mutual exchange process. However, no evidence for the "spinning" of the $Pt(CO)(PR_3)$ unit was forthcoming in the earlier reported NMR studies. In furtherance of our investigations into the reactivity of complex 1, we herein report details of the dynamic behavior of 1 and other related triosmium–platinum clusters.

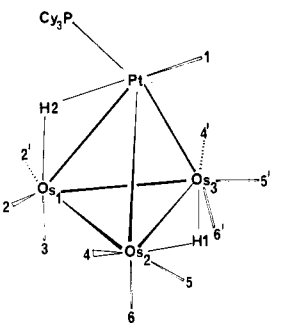

1

Results and Discussion

Dynamic Behavior of 1. The variable-temperature ^{13}C NMR spectrum of 1 is shown in Figure 1, with the parameters at 197 K given in Table I. In accordance with the effective C_s symmetry found in 1,[1] the expected six carbonyl resonances (ratio 2:2:2:1:2:1) were observed at the low-temperature limit. All signals except resonance e

(1) Farrugia, L. J.; Howard, J. A. K.; Mitrprachachon, P.; Stone, F. G. A.; Woodward, P. *J. Chem. Soc., Dalton Trans.* **1981**, 155.
(2) (a) Wade, K. *Adv. Inorg. Chem. Radiochem.* **1976**, *18*, 1. (b) Lauher, J. W. *J. Am. Chem. Soc.* **1978**, *100*, 5305. (c) Mingos, D. M. P. *Acc. Chem. Res.* **1984**, *17*, 311.
(3) (a) Mingos, D. M. P.; Wardle, R. W. M. *Transition Met. Chem. (Weinheim, Ger.)* **1985**, *10*, 441. (b) Evans, D. G.; Mingos, D. M. P. *J. Organomet. Chem.* **1982**, *240*, 321.
(4) Schilling, B. E. R.; Hoffmann, R. *J. Am. Chem. Soc.* **1979**, *101*, 3456.
(5) Farrugia, L. J.; Green, M.; Hankey, D. R.; Murray, M.; Orpen, A. G.; Stone, F. G. A. *J. Chem. Soc., Dalton Trans.* **1985**, 177.
(6) Farrugia, L. J.; Howard, J. A. K.; Mitrprachachon, P.; Stone, F. G. A.; Woodward, P. *J. Chem. Soc., Dalton Trans.* **1981**, 162.

0276-7333/88/2307-0859$01.50/0

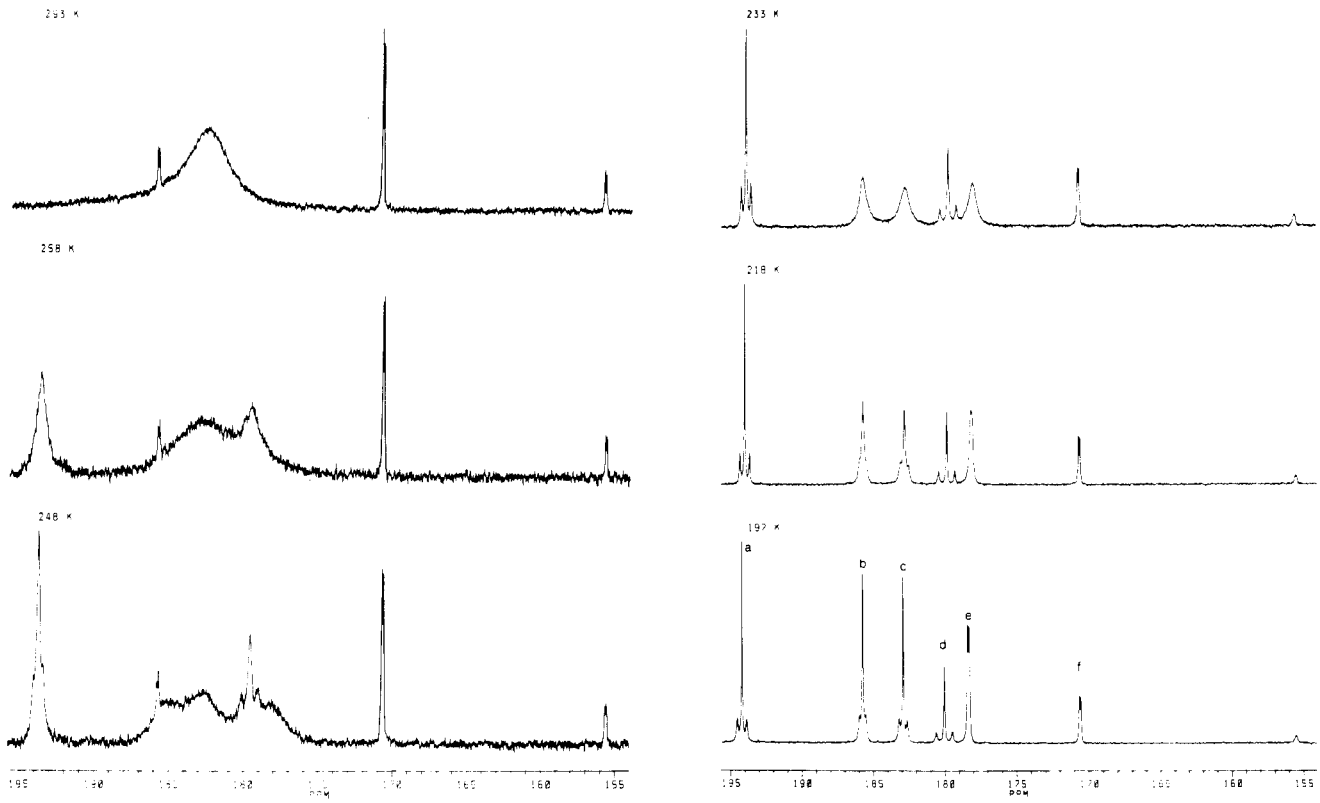

Figure 1. Variable-temperature $^{13}C\{^1H\}$ NMR spectrum of $Os_3Pt(\mu\text{-}H)_2(CO)_{10}(PCy_3)$ (1).

Table I. NMR Parameters for $Os_3Pt(\mu\text{-}H)_2(CO)_{10}(PCy_3)$ (1)

^{13}C Data[a]

reson[b]	chem shift/ppm	mult[c]	assignt	J/Hz[d] P–C	Pt–C	Os–C	H1–C	H2–C
a	194.2	s (2)	C2		33	112		w
b	185.7	s (2)	C5		22	103	w	
c	182.9	s (2)	C4		28	106	11.1	
d	180.0	s (1)	C3		57			5.0
e	178.3	d (2)	C6	5.4		117	w	
f	170.6	d (1)	C1	4.8	1517			36.0

^1H Data[e]

−6.84 (s, Os(μ-H)Os, J(Pt–H) = 6.5 Hz)
−8.47 (d, Os(μ-H)Pt, J(Pt–H) = 590, J(P–H) = 12.4 Hz)

[a] 197 K, CD_2Cl_2/CH_2Cl_2, 1:1. [b] Figure 1. [c] Multiplicites based on ^1H-decoupled spectra, relative intensities in parentheses. [d] Coupling to ^{195}Pt and ^{187}Os; w indicates small unresolved coupling. [e] 233 K, CD_2Cl_2, ppm relative to TMS.

display resolvable coupling to ^{195}Pt; the value observed for f indicates this signal is due to carbonyl C1 on the Pt atom. The high frequency Pt satellite of this resonance is obscured by signal b at the lower temperatures but becomes clearly visible on warming. The S/N ratio was sufficiently high to observe satellites due to $^1J(^{13}C\text{–}^{187}Os)$ spin–spin coupling (^{187}Os, $I = {}^1/_2$, 1.64% natural abundance). These were of the expected intensity and were symmetrically disposed about the central resonance. The magnitudes recorded in this paper fall in the narrow range 98–117 Hz. Koridze et al.,[7a] using ^{187}Os-enriched samples of $Os_3(CO)_{12}$ and $[Os_3(\mu\text{-}H)(CO)_{12}]^+$, have reported $^1J(^{13}C\text{–}^{187}Os)$ couplings in the range 84–121 Hz. During the course of this work Gallop et al.[7b] have observed similar couplings (range 84–123 Hz) in a series of osmium clusters with natural abundance ^{187}Os.

Selective ^1H decoupling in the hydride region allows assignment of the resonances (Table I). We assume that the weak and unresolved splittings are due to cis ^2J(H–C) couplings, which in these systems are smaller than the corresponding trans couplings.[8] Resonance d is clearly due to C3, since it is of relative intensity 1 and is coupled to H2 (J(C–H) = 5.0 Hz), while c may be assigned to C4/4′ on the same basis (J(C–H) = 11.1 Hz). Resonance a is

(7) (a) Koridze, A. A.; Kizas, O. A.; Astakhova, N. M.; Petrovskii, P. V.; Grishin, Y. K. *J. Chem. Soc., Chem. Commun.* **1981**, 853. (b) Gallop, M. A.; Johnson, B. F. G.; Lewis, J. *J. Chem. Soc., Chem. Commun.* **1987**, 1831.

(8) It is commonly assumed that trans ^2J(C–H) couplings are significantly larger than cis couplings in hydrido carbonyl cluster compounds (see, for example, ref 9) and assignments frequently made on this basis. While this appears valid for osmium clusters (ref 10), it is not invariably the case, e.g., in $[Re_3(\mu\text{-}H)_3(CO)_{10}]^{2-}$ (ref 11) and $CoFe_2(\mu\text{-}H)(\mu_3\text{-}COCH_3)(CO)_7(\eta\text{-}C_5H_5)$ (ref 12).

(9) Gladfelter, W. L.; Geoffroy, G. L. *Inorg. Chem.* **1980**, *19*, 2579.

(10) (a) Keister, J. B.; Shapley, J. R. *Inorg. Chem.* **1982**, *21*, 3304. (b) Chi, Y.; Shapley, J. R.; Churchill, M. R.; Li, Y.-J. *Inorg. Chem.* **1986**, *25*, 4165. (c) Gavens, P. D.; Mays, M. J. *J. Organomet. Chem.* **1978**, *162*, 389. (d) Aime, S.; Osella, D.; Milone, L.; Rosenberg, E. *J. Organomet. Chem.* **1981**, *213*, 207.

(11) Beringhelli, T.; D'Alphonso, G.; Molinari, H. J. *J. Organomet. Chem.* **1985**, *295*, C35.

(12) Aitchison, A. A.; Farrugia, L. J. *Organometallics* **1986**, *5*, 1103.

weakly coupled to H2 and is thus assigned to C2/2′. The remaining resonances b and e are assigned to C5/5′ and C6/6′ respectively on the basis of ^{195}Pt and ^{31}P couplings and by comparison with the unambiguous evidence obtained for the protonated complex $[Os_3Pt(\mu\text{-}H)_3(CO)_{10}(PCy_3)]^+$ (see below). On warming from 197 K resonances b, c, and e broaden initially, while the other signals remain sharp, indicating that the first fluxional process (process A) involves only a localized scrambling of the carbonyls C4/4′, C5/5′, and C6/6′ by $Os(CO)_3$ group rotation. Above 233 K a second fluxional process (process B) begins, which permutes all nine Os-bound CO ligands, and gives rise to a broad resonance centered at 182.6 ppm (293 K). The Pt-bound CO is clearly not involved in this exchange and remains sharp throughout. From a line-shape analysis below 233 K (where process B is not significantly operative) we obtain for process A $\Delta G^{\ddagger}_{233}$ = 49.7(5) kJ mol^{-1}. The five-site exchanging system above 233 K is too complex to analyze by using these methods.[13]

The ^{195}Pt satellites on resonance f are noticeably sharper at higher temperatures, an effect attributed to the relaxation of the ^{195}Pt nucleus[14] (believed to be dominated by the chemical shift anisotropy mechanism,[15] which is more efficient at lower temperatures). On warming above 333 K resonance f broadens and is no longer detectable at 393 K. A final exchange process thus scrambles all 10 carbonyls. Due to sample decomposition we were unable to obtain fast exchange spectra, in which averaged ^{195}Pt and ^{187}Os couplings might prove informative.

A previous variable-temperature ^{1}H NMR study[1] on the hydride exchange in the $(t\text{-Bu})_2$MeP analogue of 1 gave an approximate value for $\Delta G^{\ddagger}$ of 58 (2) kJ mol^{-1} from the observed coalescence temperature at 100 MHz. Line-shape analysis of the same process in 1 at 200 MHz was undertaken to provide more accurate thermodynamic data. Observed and calculated spectra are shown in Figure 2. The Os(μ-H)Os resonance (−6.84 ppm, 233 K) has a small coupling to ^{195}Pt (6.5 Hz), and accurate simulation (particularly of the spectrum at 283 K) was only feasible by assuming the low-frequency ^{195}Pt satellite of the Os(μ-H)Os resonance was exchanging with the high-frequency ^{195}Pt satellite of the Os(μ-H)Pt signal. This shows that the coupling constants ^1J(Pt–H2) and ^2J(Pt–H1) are of opposite sign.

The chemical shift separation between the Os(μ-H)Os and Os(μ-H)Pt sites is temperature-dependent, and at 313 K and above, the near coincidence in chemical shifts of the high-frequency ^{195}Pt satellite of the Os(μ-H)Pt resonance and the low-frequency ^{195}Pt satellite of the Os(μ-H)Os signal results in these two satellites being at the fast-exchange limit. This is responsible for the sharp doublet seen at these temperatures. The variable-temperature spectrum of 1 illustrates the phenomenon of differing coalescence temperatures for the different satellite sets, due to their different effective chemical shift separations. The couplings observed on this sharp doublet are the *averaged* couplings that would also be observable on the central resonance (i.e., that due to the non-^{195}Pt-containing isotopomer) in the fast exchange limit. The ^{31}P

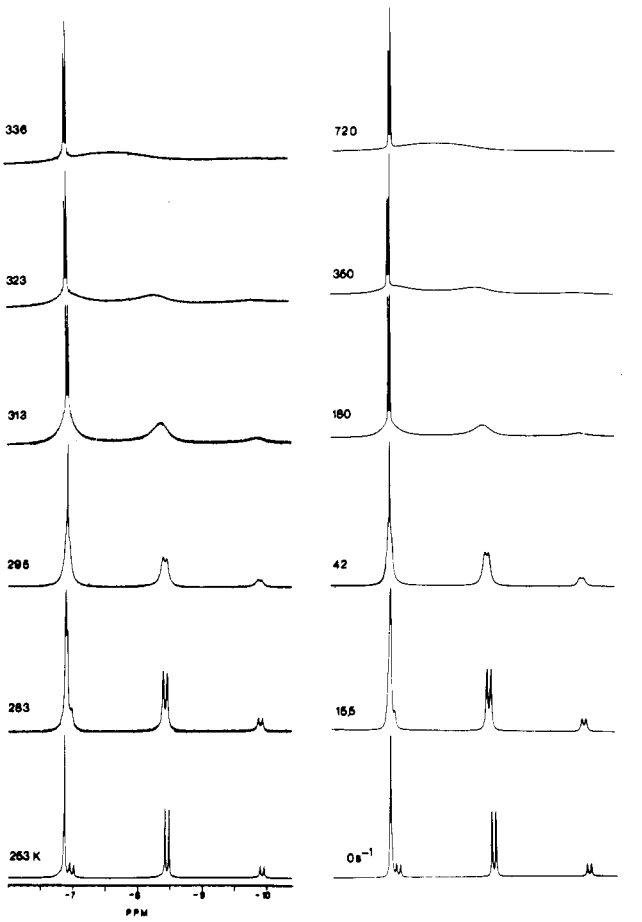

Figure 2. Observed (temperature/K) and simulated (rates/s^{-1}) variable-temperature ^{1}H NMR spectra of $Os_3Pt(\mu\text{-}H)_2(CO)_{10}(PCy_3)$ (1) in hydride region.

coupling (J = 6.4 Hz) is half that observed for the Os(μ-H)Pt resonance at slow exchange.

In addition, an *averaged* coupling to ^{187}Os is observed on this doublet as a set of ^{187}Os satellites at the base of the signal. Since in the static structure of 1 Os2 and Os3 are equivalent and Os1 is chemically distinct, two sets of *averaged* couplings of the hydrides to the ^{187}Os nuclei might be expected, with separations (based on slow exchange ^{187}Os couplings) of $[^1J(Os1\text{–}H2) + {}^2J(Os1\text{–}H1)]/2$ (= J^1_{av}) and $[^1J(Os2/3\text{–}H1) + {}^2J(Os2/3\text{–}H2)]/2$ (= $J^{2/3}_{av}$) and with relative intensities of 1:2, respectively. If the two *averaged* couplings are of similar magnitude, then only one set would be seen, as is observed. Alternatively if our proposed mechanism (see below) is correct and all Os nuclei become chemically equivalent, only one *averaged* coupling to ^{187}Os is expected, at the weighted mean of the above couplings [i.e. $^1/_3(2J^{2/3}_{av} + J^1_{av})$]. However, in view of the low natural abundance of ^{187}Os and our lack of observation of static ^{187}Os–hydride couplings in the slow exchange spectra of 1, these subtle differences in averaged couplings cannot safely be distinguished. One-bond *static* ^{187}Os–^{1}H couplings in a number of other hydride-bridged osmium clusters have been observed in the range 25–35 Hz,[16-18] and the corresponding ^2J couplings, though probably of opposite sign, are likely to be close to zero.[19] The observed

(13) The program DNMR3 allows a maximum four-site exchange; i.e. [ABCD] ⇌ [EFGH].

(14) Brady, F.; Matthews, R. W.; Forster, M. J.; Gillies, D. G. *J. Chem. Soc., Chem. Commun.* **1981**, 911.

(15) (a) Doddrell, D. M.; Barron, P. F.; Clegg, D. E.; Bowie, C. *J. Chem. Soc., Chem. Commun.* **1982**, 575. (b) Lallemand, J.-Y.; Soulié, J.; Chottard, J.-C. *J. Chem. Soc., Chem. Commun.* **1980**, 436. (c) Dechter, J. J.; Kowalewski, J. *J. Magn. Reson.* **1984**, *59*, 146. (d) Benn, R.; Buch, H. M.; Reinhardt, R.-D. *Magn. Reson. Chem.* **1985**, *23*, 559. For evidence that spin rotation is the dominant mechanism for ^{195}Pt relaxation in Pt(IV) complexes see ref 60.

(16) Koridze, A. A.; Kizas, O. A.; Kolobova, N. E.; Petrovskii, P. V.; Fedin, E. I. *J. Organomet. Chem.* **1984**, *265*, C33.

(17) Holmgren, J. S.; Shapley, J. R.; Belmonte, P. A. *J. Organomet. Chem.* **1985**, *284*, C5.

(18) Constable, E. C.; Johnson, B. F. G.; Lewis, J.; Pain, G. N.; Taylor, M. J. *J. Chem. Soc., Chem. Commun.* **1982**, 754.

(19) $^2J(^{187}Os\text{–}H)$ has been measured as 1.0 Hz in $^{187}Os(\mu\text{-}H)_2(CO)_{10}$ (ref 16).

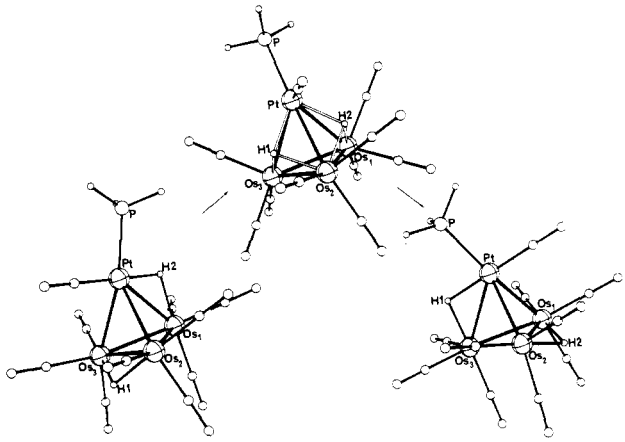

Figure 3. Proposed mechanism for the process B exchange of hydride and carbonyl ligands in complex 1.

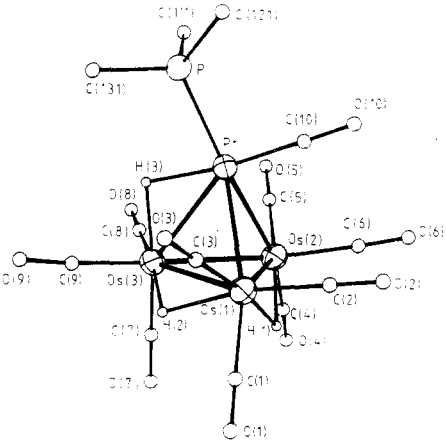

Figure 4. Molecular geometry and atomic labeling scheme for the complex cation $[Os_3Pt(\mu\text{-}H)_3(CO)_{10}(PCy_3)]^+$ (2).

averaged ^{187}Os coupling of 18.5 Hz, on the sharp doublet resonance seen above 313 K, is therefore reasonable.

The thermodynamic parameters for the hydride exchange ($\Delta G^{\ddagger}_{295}$ = 63.1 (5) kJ mol^{-1}; $\Delta H^{\ddagger}$ = 55 (1) kJ mol^{-1}; $\Delta S^{\ddagger}$ = −27 (3) J mol^{-1} K^{-1}) indicate a higher energy process than process A observed in the ^{13}C spectrum. We suggest, however, that it is linked to process B involving the total scrambling of the $Os(CO)_3$ groups. The proposed mechanism (Figure 3) invokes migration of the two hydrides across Os_2Pt faces of the tetrahedron, coupled with a synchronous rotation by 120° of the $Pt(CO)(PR_3)$ group about the centroid–Pt vector. This degenerate process exchanges the unique $Os(CO)_3$ moiety with one of the equivalent pairs of $Os(CO)_3$ groups and interchanges the two hydrides. In concert with the tripodal rotation of $Os(CO)_3$ groups that occurs at lower energy (process A), a complete permutation of all nine Os-ligated carbonyls is thus effected without inter-osmium CO exchange. Continued operation of this mechanism results in each hydride visiting Os–Os and Os–Pt edges sequentially, as implied by the ^1H data. Although this mechanism is aesthetically pleasing, other processes may be operative.[20]

Structure and Dynamic Behavior of 2. Complex 1 is formally electron-deficient but is readily protonated by $HBF_4{\cdot}Et_2O$ to give the trihydrido salt $[Os_3Pt(\mu\text{-}H)_3(CO)_{10}(PCy_3)]^+BF_4^-$ (2). The unsaturated cluster $Os_3(\mu\text{-}H)_2(CO)_{10}$ is also easily protonated,[22] as indeed are many electronprecise osmium clusters,[23] e.g. $Os_3(CO)_{12}$[7,24] and $Os_3(\mu\text{-}H)_3(\mu_3\text{-}CMe)(CO)_9$.[22] From ^1H NMR data it is evident the proton occupies an Os–Os edge, and this is also consistent with an X-ray diffraction study. Figure 4 shows the crystallographic labeling, while atomic coordinates and important metrical parameters are found in Tables II and III, respectively. The hydride ligand sites were not located crystallographically but are calculated by using potential energy minimization procedures[25] and are in agreement with the spectroscopic data. There was no evidence for disordered occupation of the Os(2)–Os(3) edge, since the calculated energy of this site was unrealistically high. In addition examination of the ligand polytope showed no

Table II. Final Positional Parameters for $[Os_3Pt(\mu\text{-}H)_3(CO)_{10}(PCy_3)]^+BF_4^-$ (2) (Fractional Coordinates) with Estimated Standard Deviations in Parentheses

	x/a	y/b	z/c
Os(1)	0.60370	0.05556 (5)	0.65452
Os(2)	0.87178 (9)	0.11082 (5)	0.64043 (4)
Os(3)	0.74424 (9)	0.02998 (5)	0.49877 (4)
Pt	0.67794 (8)	0.24876 (4)	0.56238 (4)
P	0.6212 (3)	0.3928 (3)	0.4665 (2)
O(1)	0.4927 (19)	−0.1678 (13)	0.7182 (9)
O(2)	0.5771 (18)	0.1626 (14)	0.8254 (7)
O(3)	0.3287 (14)	0.1165 (15)	0.5823 (9)
O(4)	1.1001 (15)	−0.0582 (11)	0.6660 (10)
O(5)	1.0730 (14)	0.2617 (15)	0.5506 (10)
O(6)	0.8972 (16)	0.2359 (13)	0.8055 (8)
O(7)	0.857 (2)	−0.204 (1)	0.534 (1)
O(8)	0.992 (2)	0.089 (2)	0.392 (1)
O(9)	0.551 (2)	−0.034 (1)	0.361 (1)
O(10)	0.6753 (15)	0.4017 (11)	0.7097 (7)
B	0.263 (2)	0.259 (2)	0.767 (2)
F(1)	0.2593 (17)	0.2681 (14)	0.8472 (8)
F(2)	0.3775 (12)	0.2959 (12)	0.7324 (8)
F(3)	0.231 (2)	0.160 (2)	0.738 (1)
F(4)	0.1562 (18)	0.3211 (25)	0.7388 (14)
C(1)	0.5359 (19)	−0.0885 (15)	0.6939 (10)
C(2)	0.5831 (17)	0.1240 (14)	0.7624 (11)
C(3)	0.4338 (19)	0.0930 (19)	0.6099 (10)
C(4)	1.014 (2)	0.008 (1)	0.659 (1)
C(5)	0.999 (2)	0.203 (2)	0.584 (1)
C(6)	0.8928 (18)	0.1867 (16)	0.7435 (9)
C(7)	0.818 (3)	−0.112 (2)	0.517 (1)
C(8)	0.896 (2)	0.064 (2)	0.435 (1)
C(9)	0.624 (3)	−0.013 (2)	0.414 (1)
C(10)	0.6734 (16)	0.3436 (12)	0.6538 (8)
C(111)	0.7734 (13)	0.4590 (11)	0.4248 (7)
C(112)	0.8598 (14)	0.3760 (12)	0.3744 (9)
C(113)	0.9869 (17)	0.4353 (16)	0.3390 (9)
C(114)	1.0694 (17)	0.4900 (18)	0.4073 (10)
C(115)	0.9827 (17)	0.5722 (15)	0.4599 (12)
C(116)	0.8609 (14)	0.5078 (12)	0.4963 (9)
C(121)	0.5236 (15)	0.5103 (12)	0.5171 (8)
C(122)	0.3992 (16)	0.4728 (14)	0.5591 (11)
C(123)	0.338 (2)	0.563 (2)	0.613 (1)
C(124)	0.3233 (18)	0.6780 (17)	0.5644 (11)
C(125)	0.449 (2)	0.708 (2)	0.519 (1)
C(126)	0.5067 (18)	0.6166 (14)	0.4673 (10)
C(131)	0.5346 (14)	0.3362 (12)	0.3738 (7)
C(132)	0.4045 (17)	0.2738 (16)	0.3964 (10)
C(133)	0.349 (2)	0.215 (2)	0.316 (1)
C(134)	0.330 (2)	0.294 (2)	0.245 (1)
C(135)	0.461 (2)	0.359 (2)	0.228 (1)
C(136)	0.516 (2)	0.422 (2)	0.303 (1)
H(1)	0.76760	−0.00070	0.69020
H(2)	0.60650	−0.03410	0.56050
H(3)	0.68560	0.17140	0.46330

(20) Other authors have proposed terminal hydride intermediates in exchange processes involving μ_2-hydrides (see for example ref 21).
(21) Shapley, J. R.; Richter, S. I.; Churchill, M. R.; Lashewycz, R. A. *J. Am. Chem. Soc.* **1977**, *99*, 7384.
(22) Bryan, E. G.; Jackson, W. G.; Johnson, B. F. G.; Kelland, J. W.; Lewis, J.; Schorpp, K. T. *J. Organomet. Chem.* **1976**, *108*, 385.
(23) Deeming, A. J. *Adv. Organomet. Chem.* **1986**, *26*, 1.
(24) (a) Deeming, A. J.; Johnson, B. F. G.; Lewis, J. *J. Chem. Soc. A* **1970**, 2967. (b) Knight, J.; Mays, M. J. *J. Chem. Soc. A* **1970**, 711.
(25) Orpen, A. G. *J. Chem. Soc., Dalton Trans.* **1980**, 2509.

Table III. Important Bond Lengths (Å) and Bond Angles (deg) for $[Os_3Pt(\mu\text{-}H)_3(CO)_{10}(PCy_3)]^+BF_4^-$ (2)

Bond Lengths				
Os(1)–Os(2)	2.747 (1)	[2.789 (1)][a]	Os(1)–C(3)	1.89 (2)
Os(1)–Os(3)	2.891 (1)	[2.741 (1)]	Os(2)–C(4)	1.87 (2)
Os(2)–Os(3)	2.790 (1)	[2.777 (1)]	Os(2)–C(5)	1.90 (2)
Pt–Os(1)	2.812 (1)	[2.832 (1)]	Os(2)–C(6)	1.90 (2)
Pt–Os(2)	2.819 (1)	[2.791 (1)]	Os(3)–C(7)	1.85 (3)
Pt–Os(3)	2.845 (1)	[2.863 (1)]	Os(3)–C(8)	1.87 (3)
Pt–P	2.366 (4)		Os(3)–C(9)	1.89 (3)
Pt–C(10)	1.85 (1)		P–C(111)	1.83 (1)
Os(1)–C(1)	1.93 (2)		P–C(121)	1.87 (2)
Os(1)–C(2)	1.93 (2)		P–C(131)	1.85 (1)
C–O(carbonyl) 1.15 [1] (mean)				
Bond Angles				
Os(1)–Pt–Os(2)	58.4 (1)		Pt–Os(2)–Os(1)	60.7 (1)
Os(1)–Pt–Os(3)	61.5 (1)		Pt–Os(2)–Os(3)	60.9 (1)
Os(2)–Pt–Os(3)	59.0 (1)		Os(1)–Os(2)–Os(3)	62.9 (1)
Pt–Os(1)–Os(2)	60.9 (1)		Pt–Os(3)–Os(1)	58.7 (1)
Pt–Os(1)–Os(3)	59.8 (1)		Pt–Os(3)–Os(2)	60.0 (1)
Os(2)–Os(1)–Os(3)	59.3 (1)		Os(1)–Os(3)–Os(2)	57.8 (1)
Os(2)–Os(3)–C(8)	90.8 (7)		Os(3)–Os(2)–C(5)	95.8 (6)
P–Pt–C(10)	95.1 (5)		Pt–H(3)–Os(3)	101
P–Pt–H(3)	78		Os(1)–H(1)–Os(2)	96
H(3)–Pt–C(10)	173		Os(1)–H(2)–Os(3)	103
Pt–C(10)–O(10)	178 (2)		H(1)–Os(1)–C(3)	172
Os(2)–Os(3)–C(9)	167.8 (8)		H(1)–Os(2)–C(5)	170
H(3)–Os(3)–C(7)	170		Os(3)–Os(2)–C(6)	158.6 (6)
H(2)–Os(3)–C(8)	168		H(2)–Os(1)–C(2)	169
Os–C–O = 176.7 [1] (mean)				

[a] Values in square parentheses are those corresponding distances in complex 1 (ref 1).

suitable "hole" along this edge (Table III). As expected, apart from the perturbation introduced by the hydride H(2), complex 2 has remarkably similar geometry to that of 1,[1] and it is interesting to compare corresponding metal–metal vectors given in Table III. Apart from the Os(1)–Os(3) bond, inter-metal separations in the two complexes differ by only 0.02–0.04 Å. The increase in the Os(1)–Os(3) separation (2.741 (1) Å in 1 and 2.891 (1) Å in 2) can be ascribed to the bond lengthening effect of the hydride.[26] Complex 1 has an effective mirror plane,[1] but the protonation of the Os(1)–Os(3) edge removes this symmetry element rendering 2 chiral.

The presence of two Os(μ-H)Os units in 2 allows an internal comparison of these hydride-bridged vectors. The mean value of this vector found in several tetrahedral MOs_3 clusters[27] (where M is a third-row transition metal) is 2.954 Å (range 2.922 (3)–3.005 (1) Å) and is slightly greater than the Os(1)–Os(3) separation of 2.891 (1) Å. The Os(1)–Os(2) distance of 2.747 (1) Å is, however, anomalously short and compares with that found in 1 (2.789 (1) Å). It has been suggested that the unsaturation in 1 may be localized along this edge[6] and the two distinct Os(μ-H)Os separations in 2 tend to corroborate this viewpoint.

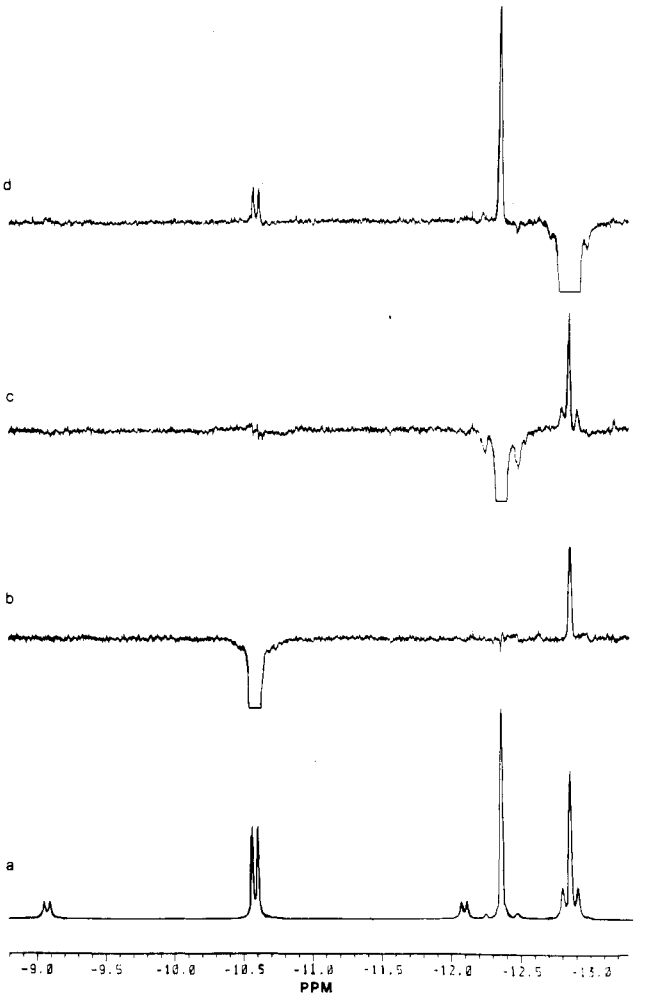

Figure 5. ^1H NOE difference spectra for $[Os_3Pt(\mu\text{-}H)_3(CO)_{10}(PCy_3)]^+BF_4^-$ (2) in hydride region: (a) off-resonance irradiation; (b) irradiation at −10.58 ppm (c) irradiation at −12.37 ppm; (d) irradiation at −12.86 ppm.

The high-field region of the ^1H NMR spectrum of 2 shown in Figure 5a displays the expected three resonances, the signal at −10.58 ppm clearly due to the Os(μ-H)Pt proton H(3) [J(P–H) = 8.0, J(Pt–H) = 603 Hz]. Assignment of the two Os(μ-H)Os resonances was obtained from NOE difference spectra, parts b–d of Figure 5. The calculated[25] internuclear separations of the hydrides are for H(1)–H(2), 2.67, H(1)–H(3), 4.27, and H(2)–H(3), 2.98 Å, with likely errors in the region of ±0.2 Å.[35] Irradiation of the resonance due to H3 at −10.58 ppm results in 2.8% enhancement at −12.86 ppm, while irradiation at −12.37 ppm enhances the signal at −12.86 ppm by 3.4%. In addition a 1.4% enhancement at −10.58 ppm and a 5% enhancement at −12.37 ppm are obtained by irradiation at −12.86 ppm, confirming that this latter signal is due to H2. In view of this unambiguous assignment several observations are worthy of note. (a) The only ^{187}Os–H coupling observed was for H1, with a single satellite of 46 Hz splitting. This implies similar J values for the two inequivalent osmium nuclei Os1 and Os2. The magnitude of the coupling constant is outside the usual observed range (25–35 Hz)[16–18] but similar to that seen (48 Hz) in $Os_3(\mu$-

(26) Teller, R. G.; Bau, R. *Struct. Bonding (Berlin)* **1981**, *44*, 1.

(27) Hydride-bridged Os–Os distances are 2.964 (2) Å (mean) in $Os_4(\mu\text{-}H)_4(CO)_{12}$ (ref 28), 2.932 (2) Å in $Os_3W(\mu\text{-}H)(CO)_{12}(\eta\text{-}C_5H_5)$ (ref 29), 2.941 (2) Å in $Os_3W(\mu\text{-}H)_3(CO)_{11}(\eta\text{-}C_5H_5)$ (ref 30), 2.987 (4) Å (mean) in $Os_3Pt(\mu\text{-}H)_4(CO)_{10}(PCy_3)$ (ref 5), 2.947 and 2.975 Å (mean) in $Os_3Pt(\mu\text{-}H)_2(\mu\text{-}CH_2)(CO)_{10}(PCy_3)$ (ref 5), 2.922 (3) Å in $Os_3W(\mu\text{-}H)(\mu_3\text{-}\eta^2\text{-}C_2tol_2)(CO)_{10}(\eta\text{-}C_5H_5)$ (ref 31), 2.964 (2) Å in $Os_3Re(\mu\text{-}H)_5(CO)_{12}$ (ref 32), 2.925 (3) and 2.934 (3) Å in $Os_3Ir(\mu\text{-}H)_3(CO)_{11}(PPh_3)$ (ref 33), and 3.005 (1) Å in $Os_3Ir(\mu\text{-}H)_2(\mu\text{-}Cl)(CO)_{10}(PPh_3)$ (ref 34).

(28) Johnson, B. F. G.; Lewis, J.; Raithby, P. R.; Zuccaro, C. *Acta Crystallogr. Sect. B: Struct. Crystallogr. Cryst. Chem.* **1981**, *B37*, 1728.

(29) Churchill, M. R.; Hollander, F. J. *Inorg. Chem.* **1979**, *18*, 843.

(30) Churchill, M. R.; Hollander, F. J. *Inorg. Chem.* **1979**, *18*, 161.

(31) Park, J. T.; Shapley, J. R.; Churchill, M. R.; Bueno, C. *J. Am. Chem. Soc.* **1983**, *105*, 6182.

(32) Churchill, M. R.; Hollander, F. J.; Lashewycz, R. A.; Pearson, G. A.; Shapley, J. R. *J. Am. Chem. Soc.* **1981**, *103*, 2430.

(33) Johnson, B. F. G.; Lewis, J.; Raithby, P. R.; Azman, S. N.; Syed-Mustaffa, B.; Taylor, M. J.; Whitmire, K. H.; Clegg, W. *J. Chem. Soc., Dalton Trans.* **1984**, 2111.

(34) Adams, R. D.; Horvath, I. T.; Segmüller, B. E. *Organometallics* **1982**, *1*, 1537.

(35) For 36 neutron-determined cluster structures an average positional error of ±0.05 Å for the hydride ligand is obtained by using HYDEX (ref 25). The X-ray coordinates used for 2 are likely to increase this margin, but minor errors in the H–H distances do not affect the qualitative interpretation of the NOE results.

Table IV. NMR Parameters for $[Os_3Pt(\mu\text{-}H)_3(CO)_{10}(PCy_3)]^+BF_4^-$ (2)

^{13}C Data[a]

reson[b]	chem shift/ppm	mult[c]	assgnt[e]	J/Hz[d] P–C	Pt–C	Os–C	H1–C	H2–C	H3–C
a	178.3	s	C5		31	103	10.4		
b	174.5	s	C9		54	105		w	w
c	174.0	s	C8					6.7	w
d	172.6	d	C4	5.4			w		
e	171.8	s	C7		64	114		w	6.7
f	171.5	s	C6		29	104	w		
g	168.3	d	C10	5.1	1543				34.0
h	165.9	s	C3		25	98	12.7	w	
i	164.3	d	C1	8.4	17		w	w	
j	162.2	s	C2			108	w	12.1	w

^1H Data[f]

−10.58 (d, Os(μ-H)Pt, J(Pt–H) = 603, J(P–H) = 8.0 Hz)
−12.37 (dd, Os(μ-H)Os, J(Os–H) = 46, J(P–H) = 1.1 J(H–H) = 1.7 Hz)
−12.86 (dd, Os(μ-H)Os, J(P–H) = 1.7, J(H–H) = 1.7, J(Pt–H) = 21.5 Hz)

[a] 213 K, CD_2Cl_2/CH_2Cl_2, 1:1. [b] Figure 6. [c,d] As for Table I. [e] Figure 4. [f] 213 K, CD_2Cl_2, ppm relative to TMS.

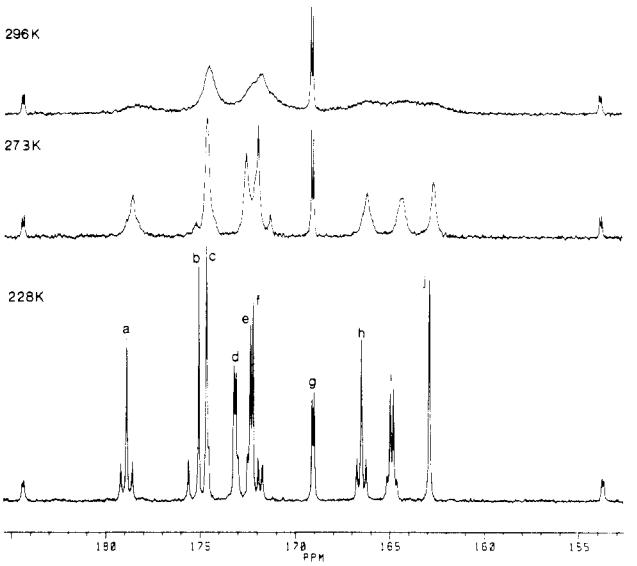

Figure 6. Variable-temperature $^{13}C\{^1H\}$ NMR spectrum of $[Os_3Pt(\mu\text{-}H)_3(CO)_{10}(PCy_3)]^+BF_4^-$ (2).

Scheme I

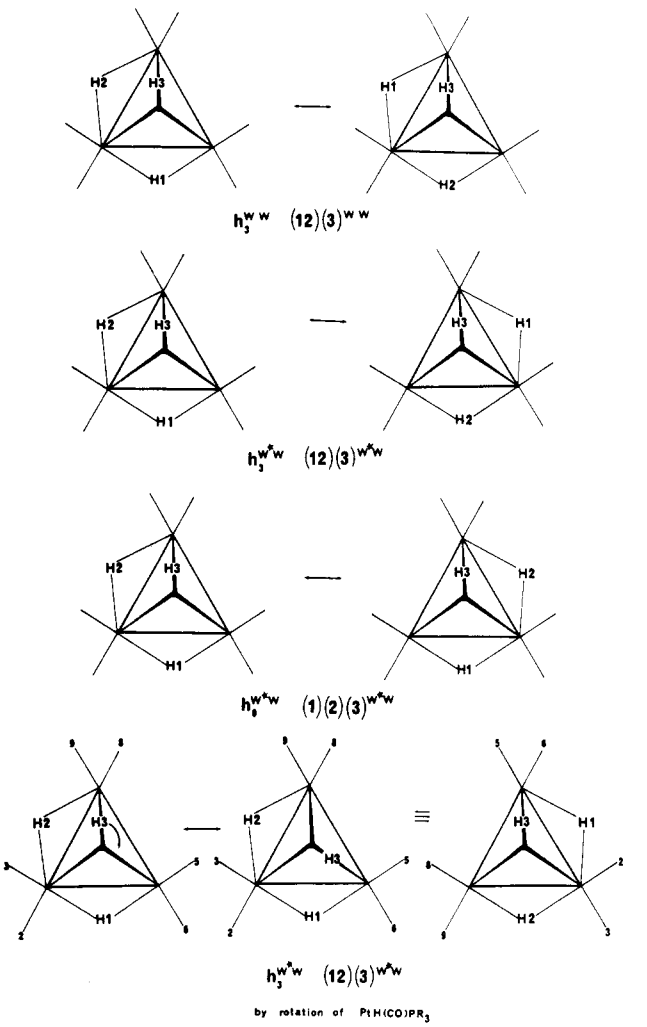

$H)_2(CO)_{10}$,[16] providing perhaps further evidence for the localization of unsaturation in 2 along the Os(1)–Os(2) vector. (b) There is a considerable shift of the hydride resonances to low frequency on protonation, particularly visible in the Os(μ-H)Os signal (−6.84 ppm in 1, −12.37 ppm in 2). (c) The hydride on the "mirror plane" in 2, i.e., H(1) has no resolvable ^{195}Pt coupling, while that due to H2 has J(Pt–H) = 21.5 Hz. Since the Os(μ-H)Os signal in 1 has only a small ^{195}Pt coupling, this may prove diagnostic of hydride location in related *tetrahedro*-Os_3Pt clusters.

On warming above 213 K the two Os(μ-H)Os resonances broaden, while that due to the Os(μ-H)Pt proton remains sharp. From a line-shape analysis of this two-site exchange we obtain ΔG^*_{293} = 62.7 (5) kJ mol^{-1}. Considering only the hydride ligand sites and using the notation of Klemperer,[36] only those permutations $h_3{}^{WW}$ = (12)(3)^{WW} (exchange of H1 and H2 within the same configuration) and $h_3{}^{W*W}$ = (12)(3)^{W*W} (exchange of H1 and H2 coupled with simultaneous racemization) are compatible with the data (Scheme I). These two permutations are indistinguishable in the ^1H NMR spectrum. The permutation $h_0{}^{W*W}$ = (1)(2)(3)^{W*W} (i.e., racemization of the cluster by H2 migration with *no* exchange of the hydride environments), which is an "invisible" process in the ^1H NMR spectrum, is, however, detectable in the ^{13}C experiment, and this latter experiment also allows differentiation between $h_3{}^{WW}$ and $h_3{}^{W*W}$.

The variable-temperature ^{13}C NMR spectrum of 2 is shown in Figure 6, with relevant parameters given in Table IV. Distinct resonances for all 10 inequivalent carbonyls were observed at 228 K. The assignments are based on the resolved and unresolved couplings to the hydride lig-

(36) Klemperer, W. G. In *Dynamic Nuclear Magnetic Resonance Spectroscopy*; Cotton, F. A., Jackman, L. M., Eds.; Academic: New York, 1975; Chapter 2.

Table V. NMR Parameters for $Os_3Pt(\mu\text{-}H)_2(CO)_{11}(PCy_3)$ (3)

^{13}C Data[a]

reson[b]	chem shift/ppm	mult[c]	assgnt[e]	J/Hz[d] P–C	Pt–C	Os–C	H1–C	H2–C
a	179.5	s (6)	C1, C5, C7, C8–C10		294	48,36	3.2	
b	177.1	s (1)	C11			115		
c	176.3	s (1)	C3		120		11.2	3.1
d	174.4	d (1)	C6	2.2	7	114		6.9
e	172.5	s (1)	C2			109	4.1	3.6
f	171.1	s (1)	C4		4	107	4.6	9.6

^1H Data[f]

−11.65 (d, Os(μ-H)Pt, J(Pt–H) = 503, J(P–H) = 11 Hz)
−17.60 (d, Os(μ-H)Os, J(Pt–H) = 31, J(P–H) = 2 Hz)

[a] 233 K, CD_2Cl_2/CH_2Cl_2, 1:1. [b] Figure 8. [c,d] As for Table I. [e] Figure 7. [f] 223 K, $CDCl_3$, ppm relative to TMS.

ands (Table IV). Thus resonance a has a 10.4 Hz coupling to H1 and no visible coupling to the other hydrides and is thus assigned to C5 trans to H1. Resonance h also has a significant coupling of 12.7 Hz to H1 but is weakly coupled to H2 and is thus assigned to C3 which is trans to H1 and cis to H2. Similar reasoning leads to the other assignments, with the remaining ambiguity in assignment of resonances d and f to the carbonyl pair C4/C6 resolved by the magnetization transfer experiments (see below). ^{187}Os couplings were observed on all singlet resonances except c, and ^{195}Pt couplings resolvable on all signals apart from c, d, and j. On warming to 273 K (Figure 6) all resonances except e and g broaden, suggesting that **2** is racemizing and acquiring a time-averaged mirror plane. This is compatible with both hydride permutations h_3^{W*W} and h_0^{W*W}. Further information on the CO exchange at 253 K was afforded by magnetization transfer studies using a DANTE pulse train[37] to excite resonances selectively. Inversion of resonance a (C5) results in saturation transfer to h (C3). No transfer is seen to C1 or C4 at 253 K, indicating there is *no significant tripodal rotation* of these $Os(CO)_3$ groups. This is in contrast to the situation seen in **1** where such a process is the lowest energy one and already operative at 218 K. Since inversion of j leads to exclusive spin transfer to f and inversion of d to transfer to i, the respective assignments of d and f to C4 and C6 are obtained. Due to the proximity of resonances b and c, it was not possible to demonstrate spin transfer between C8 and C9. Permutation h_3^{W*W} thus accounts for both the hydride and carbonyl exchange behavior and *may* be the sole operative process[38] at this temperature. However we cannot preclude contributions from h_3^{WW} and h_0^{W*W} without further quantitative studies. Operation of the hydride permutation h_3^{W*W} *solely* by rotation of the PtH(CO)(PR_3) moiety is ruled out by the ^{13}C data. We note that Keister et al.[39] have recently reported two distinct hydride exchange processes in the complex $Ru_3(\mu\text{-}H)_2(\mu_3\text{-}\eta^2\text{-}CHC(O)OCH_3)(CO)_9$ which correspond to our permutations h_0^{W*W} and h_3^{WW} and which have significantly different energies.

DANTE experiments carried out at the higher temperature of 263 K reveal that on inversion of a, in addition to spin transfer to h, saturation is also carried to b, c, f, and j but none to d or i. This implies a further exchange process whereby the six pseudoequatorial carbonyls C2, C3, C5, C6, C8, and C9 are permuted with each other but

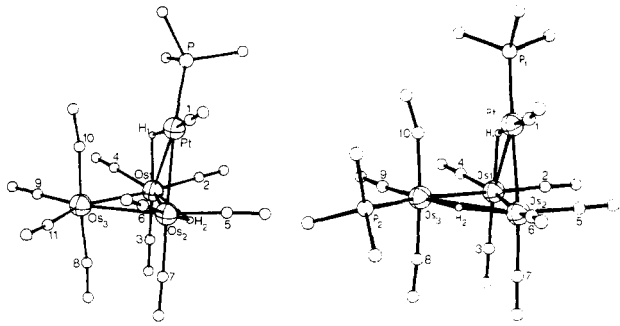

Figure 7. Geometries of $Os_3Pt(\mu\text{-}H)_2(CO)_{11}(PCy_3)$ (**3**) and $Os_3Pt(\mu\text{-}H)_2(CO)_{10}(PCy_3)_2$ (**4**) showing the atomic labeling scheme.

not with the pseudoaxial ligands C1, C4, or C7. Such a process is consistent with a polytopal rotation of the $PtH(CO)(PR_3)$ fragment about the Os_3 triangle coupled with hydride migration, although other mechanisms, e.g., a "merry-go-round" CO exchange[40] cannot be ruled out. Figure 6 clearly shows however that even at 296 K the Pt-bound CO (resonance g) is not involved in exchange with the Os-ligated carbonyls. Rotation of a PtH(CO)-(PR_3) fragment with retention of stereochemical integrity has been previously observed[42] as a fluxional process in $[PtRh_2(\mu\text{-}H)(\mu\text{-}CO)_2(CO)(PPh_3)(\eta\text{-}C_5Me_5)_2]^+BF_4^-$.

Dynamic Behavior of 3. The apparent stereochemical rigidity of the $Pt(CO)(PR_3)$ unit in complexes **1** and **2** led us to investigate the fluxional behavior of the related butterfly adducts $Os_3Pt(\mu\text{-}H)_2(CO)_{10}(PCy_3)(L)$ (**3**, L = CO; **4**, L = PCy_3), which also possess such a fragment. The X-ray structure[5] of complex **3** is shown in Figure 7 with the nuclear labeling. The ^{13}C NMR spectrum of **3** at 233 K (Figure 8) shows that only six resonances, a–f (intensity ratio 6:1:1:1:1:1, respectively), are observed for the 11 chemically distinct CO environments. The intensity 6 resonance a displays coupling to ^{195}Pt (294 Hz) and has two sets of ^{187}Os satellites. The retention of coupling requires that those carbonyls involved in the exchange and the ^{195}Pt and ^{187}Os nuclei to which they are coupled remain in the same molecules during any averaging process. The most straightforward explanation for these couplings and the variable-temperature spectra (Figure 9) is that a low-energy exchange averages six CO sites in complex **3**. The relatively small ^{195}Pt coupling of 294 Hz is consistent with

(37) Morris, G. A.; Freeman, R. *J. Magn. Reson.* **1978**, *29*, 433.
(38) A crude estimate of ca. 19 s^{-1} for the exchange rate at 273 K is obtained from the observed coalescence of signals b and c in the ^{13}C spectrum, and this compares favorably with the rate of 13 s^{-1} at the same temperature calculated from band-shape analysis on the ^1H spectrum.
(39) Churchill, M. R.; Janik, T. S.; Duggan, T. P.; Keister, J. B. *Organometallics* **1987**, *6*, 799.
(40) The planar "merry-go-round" mechanism (ref 41) requires the formation of CO bridges, and since two of the Os–Os edges are already hydride-bridged, we consider such a process of too high energy.
(41) Band, E.; Muetterties, E. L. *Chem. Rev.* **1978**, *78*, 639.
(42) Green, M.; Howard, J. A. K.; Mills, R. N.; Pain, G. N.; Stone, F. G. A.; Woodward, P. *J. Chem. Soc., Chem. Commun.* **1981**, 869.

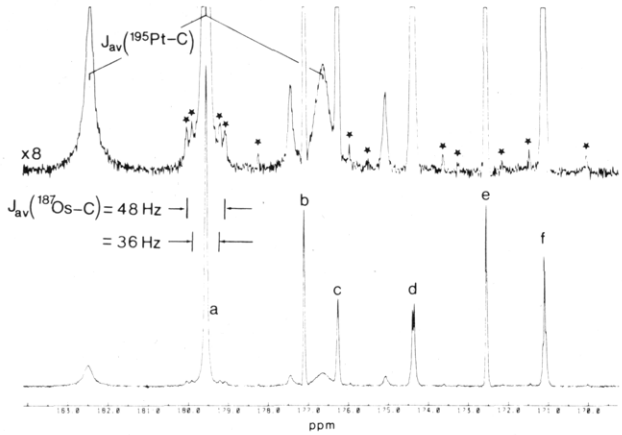

Figure 8. 50.3-MHz $^{13}C\{^1H\}$ NMR spectrum (233 K) of $Os_3(\mu\text{-}H)_2(CO)_{11}(PCy_3)$ (**3**) showing the averaged couplings to ^{195}Pt and ^{187}Os. Lorentz/Gaussian line narrowing is used to enhance resolution of ^{187}Os satellites, shown by the asterisk (*).

Scheme II

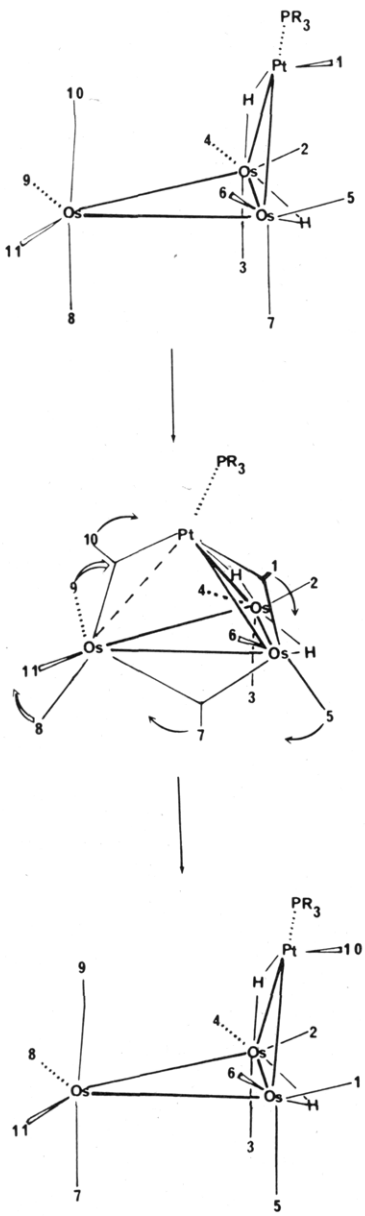

a process permuting site 1 on Pt with five Os carbonyl sites, such that each CO spends on average one-sixth of its time on the Pt center.[43] The assignments of the remaining

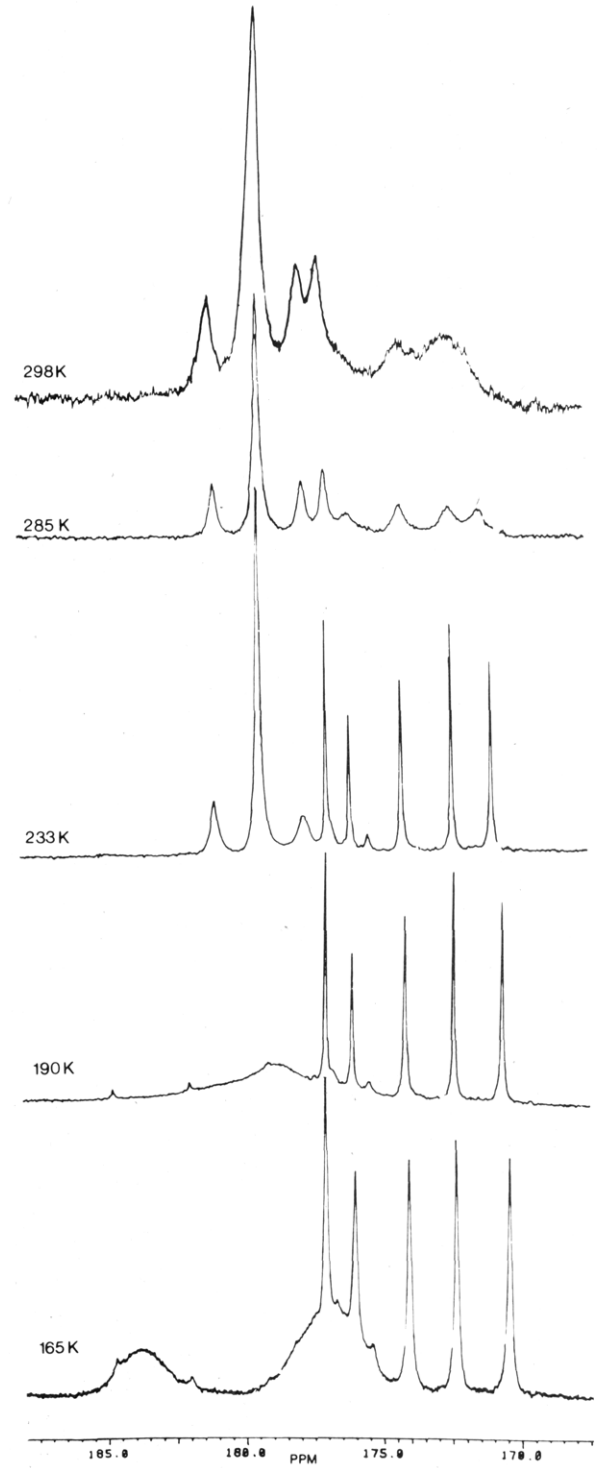

Figure 9. Variable-temperature 90.5-MHz $^{13}C\{^1H\}$ NMR spectrum of complex **3**.

signals b–e (Table V) are based on the couplings to the hydride ligands. Resonances c–f can be assigned to C3, C6, C2, and C4, respectively, on the basis of arguments outlined above for complexes **1** and **2**. Resonance b has no detectable coupling to the hydrides, and we thus attribute this to one of the carbonyls in the $Os(CO)_4$ group

(43) The coupling constant of 294 Hz is close to one-sixth of the static ^{195}Pt–C10 coupling observed in **4** (1773/6 = 295.5 Hz) and in the related adduct $Os_3Pt(\mu\text{-}H)_2(CO)_{10}(PCy_3)(CNCy)$ where the corresponding coupling is 1784 Hz (ref 44). The large one-bond coupling provides the dominant term for the *averaged* coupling.

(44) Ewing, P.; Farrugia, L. J. *Organometallics*, following paper in this issue.

on Os3. According to these assignments the five Os-bound CO ligands involved in the exchange must therefore be C5, C7, and the other three on the $Os(CO)_4$ group. The assignment of resonance b as due to C11 is by no means firm but arises from the proposed exchange mechanism and the appearance of the spectrum at 165 K (see below and Figure 9). In addition to the ^{195}Pt coupling, resonance a also displays two distinct sets of satellites due to coupling to ^{187}Os.[45] We ascribe these satellite pairs, with $J(^{187}Os–C)$ = 36 and 48 Hz, as due to *averaged* coupling of the six CO ligands to Os2 and Os3, respectively. The proposed fluxional mechanism (Scheme II) requires that each CO resides on average one-third of the time on Os2 and one-half the time on Os3. These *averaged* couplings observed are consistent with the appropriately weighted nondynamic $^{187}Os–^{13}C$ ^1J values reported in this paper and by other authors.[7] We suggest that this unusual six-site intramolecular carbonyl exchange proceeds via a transition state where there is a closo or "semicloso" metal framework and an incipient CO bridge across the two "wingtip" atoms. Such a scheme requires a considerable deformation of the metal framework and a planar "merry-go-round" process about the PtOs2Os3 face. Carbonyl C11 is in an "axial" position with respect to this face, and we tentatively suggest that this is the CO ligand in the $Os(CO)_4$ group *not* involved in the exchange.

In support of this proposal we cite the following evidence. (a) There is already an apparent weak interaction between the Pt atom and C10 in the ground-state structure of **3**, viz., the contact distance Pt···C10 = 2.97 (2) Å and Os–C10–O10 = 171 (2)°. In complex **4**[69] this interaction is slightly more pronounced (Pt···C10 = 2.880 (7) Å; Os–C10–O10 = 169.6 (6)°). (b) Although CO bridges across nonbonded metal–metal vectors are known, e.g., in $Pt_2Cl_2(dpam)_2(\mu\text{-}CO)$[46] Pt–Pt = 3.162 (4) Å, the wingtip Pt–Os distance of 3.530 (1) Å in **3** is significantly greater than usually observed in these systems. (c) There is mounting evidence that the flexing of the butterfly metal framework is a soft deformation mode,[47] and observations of low-energy skeletal rearrangements in other metal geometries are increasingly common.[48] We cite in particular the proposed fluxional behavior of $Os_3Pt(\mu_3\text{-}S)_2(CO)_9(PMe_2Ph)_2$[49] and $Os_4(CO)_{14}(PMe_3)$[50] where considerable atomic displacements of the metal centers and associated ligands are involved. (d) Complex **3** is of the structural type $Os_3(\mu\text{-}H)(\mu\text{-}X)(CO)_{10}$, and several other examples have been reported where a trigonal twist mechanism results in polytopal exchange in the unique $Os(CO)_4$ group.[10c,51–53] Particularly interesting is the observation by Aime et al.[53] that the bridging vinyl group in $Os_3(\mu\text{-}H)(\mu\text{-}PhC{=}C(H)Ph)(CO)_{10}$ promotes a selective trigonal twist exchange in the $Os(CO)_4$ group, leaving one axial CO ligand uninvolved. A similar "bridge-promoted" exchange apparently takes place in complex **3**, leaving one CO ligand uninvolved (which we assign to the equatorial site C11). In this context it is interesting to note that for μ-X = H, i.e., for $Os_3(\mu\text{-}H)_2(CO)_{10}$, the unique $Os(CO)_4$ group is rigid at accessible temperatures and only a very slow rotation (0.36 s^{-1} at 300 K) of the $Os(CO)_3$ groups is observed.[54]

Table VI. NMR Parameters for $Os_3Pt(\mu\text{-}H)_2(CO)_{10}(PCy_3)_2$ (4)

^{13}C Data[a]

reson[b]	chem shift/ ppm	mult[c]	assgnt[e]	J/Hz[d] P–C	Pt–C	H1–C	H2–C
a	185.9	d	C10	5.4	27		2.5
b	184.4	d	C8	6.1	17		2.5
c	183.2	s	C3		102	11.0	
d	183.2	d	C6	13.2			w
e	182.4	s	C7		44		3.3
f	181.0	s	C4		50	3.7	
g	180.1	d	C1	4.2	1773	28.9	
h	179.9	d	C2	2.0	19	w	
i	178.0	s	C9				5.7
j	176.8	d	C5	3.0	39		7.2

^1H Data[f]

−9.15 (d, Os(μ-H)Pt, J(Pt–H) = 582, J(P–H) = 15 Hz)
−18.30 (d, Os(μ-H)Os, J(P–H) = 11 Hz)

^{31}P Data[g]

11.4 (s, OsP)
51.5 (s, PtP, J(Pt–P) = 2528 Hz)

[a] 258 K, toluene-d_8/toluene, 1:1. [b] Figure 10. [c,d] As for Table I. [e] Figure 7. [f] 373 K, toluene-d_8, ppm relative to TMS. [g] 295 K, toluene-d_8, ^1H decoupled, ppm relative to external H_3PO_4.

From the variable-temperature spectra (Figure 9) it is evident that the six-site exchange process in **3** is of very low energy. Even at 165 K only partial resolution of the six CO ligands into two broad resonances is achieved. We suggest that the signal at 184 ppm (relative intensity 2) is due to C8 and C10, (since the axial CO ligands in $Os(CO)_4$ groups are usually the most deshielded[7,10,51]), while the broad resonance centered at 177 ppm (relative intensity ca. 4) arises from the remaining four carbonyls. Above 233 K resonances c–f broaden considerably, indicating further exchange processes, which are likely to involve rotation of the $Os(CO)_3$ units. Resonance b broadens less rapidly, consistent with its assignment as a carbonyl in the $Os(CO)_4$ group, and suggests a higher energy trigonal twist motion in this group may be occurring. Distinct signals are observed for the Os(μ-H)Os and Os(μ-H)Pt protons in the ^1H NMR spectrum at 298 K (at −17.60 and −11.65 ppm, respectively), and on warming to 348 K only a slight broadening occurs, indicating that the hydride mobility in **3** is considerably lower than in **1** or **2**. Complex **3** easily loses CO above ambient temperature to regenerate the closo unsaturated species **1**. This instability prevents accurate studies of the hydride fluxionality. At temperatures below 190 K (Figure 9) weak signals attributed to **1** are observed, presumably due to the slowing of the rate of the chemical exchange:

$$3 \rightleftharpoons 1 + CO$$

The equilibrium strongly favors **3** at these low temperatures however, complex **1** being present as a very minor component (less than 5%). The variable-temperature

(45) The axial–axial $^2J(^{13}C–^{13}C)$ couplings are ca. 30–35 Hz in these systems; see, for example: Aime, S.; Osella, D. *J. Chem. Soc., Chem. Commun.* **1981**, 300. This source of coupling can be discounted however due to the averaging process occurring.

(46) Brown, M. P.; Keith, A. N.; Manojlovic-Muir, Lj.; Muir, K. W.; Puddephatt, R. J.; Seddon, K. R. *Inorg. Chim. Acta* **1979**, *34*, L223.

(47) (a) Bogdan, P. L.; Horwitz, C. P.; Shriver, D. F. *J. Chem. Soc., Chem. Commun.* **1986**, 553. (b) Bruce, M. I.; Nicholson, B. K. *J. Organomet. Chem.* **1983**, *250*, 627. (c) Carty, A. J.; MacLaughlin, S. A.; Wagner, J. V.; Taylor, N. J. *Organometallics* **1982**, *1*, 1013.

(48) Salter, I. D. *Adv. Dynamic Stereochem.* **1987**, *2*, in press.

(49) (a) Adams, R. D.; Wang, S. *Inorg. Chem.* **1985**, *24*, 4449. (b) Adams, R. D.; Horvath, I. T.; Wang, S. *Inorg. Chem.* **1986**, *25*, 1617.

(50) Martin, L. R.; Einstein, F. W. B.; Pomeroy, R. K. *J. Am. Chem. Soc.* **1986**, *108*, 338.

(51) Bryan, E. G.; Forster, A.; Johnson, B. F. G.; Lewis, J.; Matheson, T. W. *J. Chem. Soc., Dalton Trans.* **1978**, *196*.

(52) Yeh, W.-Y.; Shapley, J. R.; Li, Y.-J.; Churchill, M. R. *Organometallics* **1985**, *4*, 767.

(53) Aime, S.; Gobetto, R.; Osella, D.; Milone, L.; Rosenberg, E.; Anslyn, E. V. *Inorg. Chim. Acta* **1986**, *111*, 95.

(54) (a) Aime, S. *Inorg. Chim. Acta* **1982**, *62*, 51. (b) Hawkes, G. E.; Randall, E. W.; Aime, S.; Osella, D.; Elliot, J. E. *J. Chem. Soc., Dalton Trans.* **1984**, 279.

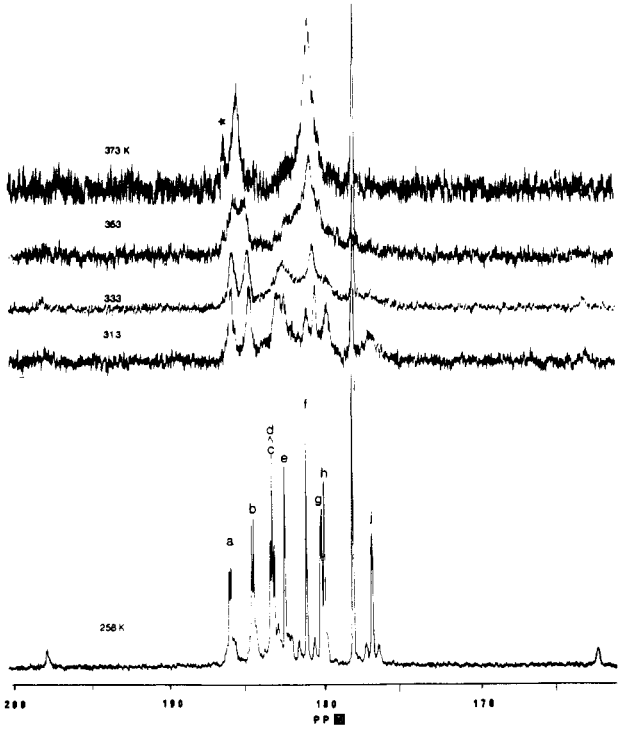

Figure 10. Variable-temperature $^{13}C\{^1H\}$ NMR spectrum of $Os_3Pt(\mu\text{-}H)_2(CO)_{10}(PCy_3)_2$ (4). The asterisk (*) denotes impurity due to decomposition.

spectra of 3 under 1-atm pressure of CO are identical with those obtained from solutions which have been purged with nitrogen. Moreover since resonances a–f all show couplings to at least one of the spin $^1/_2$ nuclei (^1H, ^{195}Pt, or ^{187}Os) present in complex 3 (see Table V), the chemical exchange between 1 and 3 involving free CO cannot be responsible for the six-site exchange observed for 3.

Dynamic Behavior of 4. In view of this novel exchange involving CO transfer between the butterfly "wingtip" metals, we were intrigued to see is such a process occurred in related species. The fluxional behavior of the adduct $Os_3Pt(\mu\text{-}H)_2(CO)_{10}(PCy_3)_2$, complex 4, was thus examined. The crystal structure of 4[69] (Figure 7) is very similar to that of the PPh_3 analogue[6] and shows that the additional phosphine is equatorially substituted on Os3, and the Os(μ-H)Os hydride is now cis to this ligand so that the hydride disposition differs slightly from that found in 3. This cis relationship between hydrides and phosphine ligands has been discussed in terms of steric preferences.[5]

The variable-temperature ^{13}C NMR spectrum of 4 is shown in Figure 10, and relevant NMR parameters are given in Table VI. It is immediately evident that 4 does not show the same low-energy six-site exchange seen in 3, and even at 295 K separate signals for the 10 chemically distinct CO's are observed. The substitution of a CO by the bulky ligand PCy_3 thus appears to block this fluxional pathway, although the presence of the μ-hydride on the Os2–Os3 edge may also play a role by hindering CO interchange between these osmium centers. Figure 10 shows, however, that higher energy exchange processes are occurring. Unfortunately assignments for 4 are not as firm as for the previous compounds. Resonance g is clearly due to C1 from the large ^{195}Pt coupling, and c can safely be assigned to C3 on the basis of the 11-Hz coupling to H1. From the fluxional behavior we assign resonance i to C9 and resonances a and b to C10 and C8 respectively. These latter two signals are the most deshielded, and both have a small ^{31}P coupling. The lack of such coupling (to P2) on the equatorial C9 resonance is somewhat surprising, though this pattern has been observed in several Os_3 clusters containing the $Os(CO)_3(PR_3)$ unit, where the axial CO ligands couple to the equatorial phosphine, but the CO cis to the phosphine shows either no coupling or an unresolved coupling.[10a,55,56] The pairs of resonance d, e and f, h may be ascribed to the carbonyl pairs C6, C7 and C2, C4, respectively, on the basis of the small couplings to H2 and H1 (see Table VI). We tentatively assign signal h to C2, with the small ^{31}P coupling due to long-range trans coupling to P2.[10a,57] From the magnitudes of the $^2J(^{195}Pt\text{–}C)$ coupling constants we suggest that resonance e is due to C7 (cf. the axial carbonyl C3, trans to Pt, has a large coupling of 102 Hz) and resonance a to C10 (on the basis of weak interaction with Pt). However, in view of the wide range of these coupling constants reported in this work (0–120 Hz) and the absence of any clear correlation with structural parameters (for example, Pt–Os–C angles), these assignments must be regarded as tentative.

Figure 10 shows that on warming all resonances except i collapse, giving at 373 K a coalesced signal at 185.7 ppm arising from a and b, a sharp signal due to i, and a broad resonance at 181.1 ppm due to the remaining CO ligands. The collapse of resonances a and b occurs at a slower rate compared to the other signals, and an approximate value for ΔG^*_{363} of 76 (2) kJ mol^{-1} is calculated from the coalescence temperature of 363 (± 5) K and the estimated chemical shift difference (44 ± 3 Hz) at this temperature. The broadening of the Pt–CO resonance implies exchange with Os–CO ligands. Rather surprisingly the ^1H NMR spectrum at 373 K shows two sharp doublets at −9.15 and −18.30 ppm due to the Os(μ-H)Pt and Os(μ-H)Os protons, respectively, indicating that there is no detectable hydride exchange in 4. These data suggest that although several fluxional processes are operative, the coordination sphere of Os3 remains stereochemically intact. Interchange of the two axial resonances a and b by rotation of the $Os_3[H(CO)_3PR_3]$ group through 180° about an axis through Os3 normal to the Os1–Os2 vector[58] (coupled with a similar rotation of the $PtH(CO)(PR_3)$ moiety to render the process degenerate) is ruled out by further magnetization transfer studies using DANTE and ^{13}C 2D exchange correlation NOESY spectroscopy.[59,60] This "double rotation" mechanism requires exchange of the Os1 and Os2 environments, and we find no evidence for carbonyl scrambling between these centers. For molecules such as complex 4 having multiple CO exchange pathways, the 2D NOESY technique (perhaps more appropriately referred to as EXSY or exchange spectroscopy[60]) is particularly attractive since in principle exchange rates between all sites are obtainable from one experiment.[59,60]

The symmetrized 2D exchange correlation NOESY spectrum for 4 (Figure 11) measured at 298 K with a mixing time of 0.15 s clearly shows off-diagonal signals between resonances a and b, indicating significant exchange at this temperature. In addition tripodal rotation of the $Os(CO)_3$ groups on Os1 and Os2 is indicated by the off-diagonal peaks between resonances c, f, and h and

(55) Deeming, A. J.; Donovan-Mtunzi, S.; Kabir, S. E.; Manning, P. J. *J. Chem. Soc., Dalton Trans.* **1985**, 1037.
(56) Johnson, B. F. G.; Lewis, J.; Reichert, B. E.; Schorpp, K. T. *J. Chem. Soc., Dalton Trans.* **1976**, 1403.
(57) Stuntz, G. F.; Shapley, J. R. *J. Am. Chem. Soc.* **1977**, *99*, 607.
(58) A similar rotation of an $ReH(CO)_4$ group in $[Re_3(\mu\text{-}H)_3(CO)_{13}]^{2-}$ has recently been postulated; see: Beringhelli, T.; D'Alphonso, G.; Molinari, H.; Mann, B. E.; Pickup, B. T.; Spencer, C. M. *J. Chem. Soc., Chem. Commun.* **1986**, 796.
(59) Hawkes, G. E.; Lian, L. Y.; Randall, E. W.; Sales, K. D.; Aime, S. *J. Chem. Soc., Dalton Trans.* **1985**, 225.
(60) Abel, E. W.; Coston, T. P. J.; Orrell, K. G.; Šik, V.; Stephenson, D. *J. Magn. Reson.* **1986**, *70*, 43.

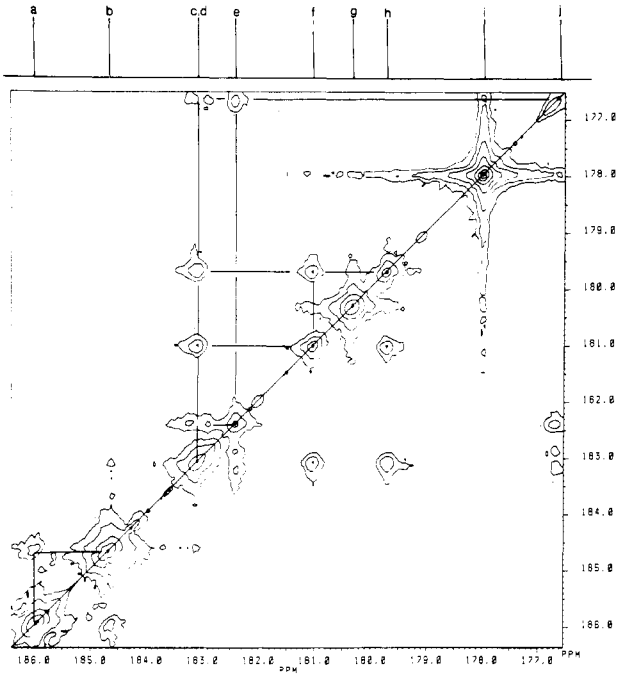

Figure 11. Symmetrized $^{13}C\{^1H\}$ 2D exchange correlation NOESY NMR spectrum for complex **4**.

between d, e, and j, respectively. There is no evidence for off-diagonal peaks between CO ligands on Os1 and those on Os2, implying no observable direct or indirect exchange at 298 K. While there is some evidence in the magnetization transfer studies for selective exchange of the Pt-bound CO with those on Os1, the 2D NOESY spectrum shows no unequivocal correlations between resonance g and any others. This implies that the Pt–CO/Os–CO exchange observed by line broadening in the variable-temperature studies occurs at higher energy than the other processes. We suggest that the a/b site exchange occurs via a planar transition state (Scheme III). Such a planar structure is seen in the equilibrium geometry of several 62-electron butterfly clusters including $Os_4(CO)_{14}(PMe_3)$[50] and $Os_3ReH(CO)_{15}$.[61] Oscillation of the structure through this planar intermediate interconverts the enantiomers of **4** and exchanges the environments of C8 and C10 while the carbonyl sites C1 and C9 are left unaffected. The Pt–CO/Os–CO exchange may also occur via the planar intermediate.

Scheme III

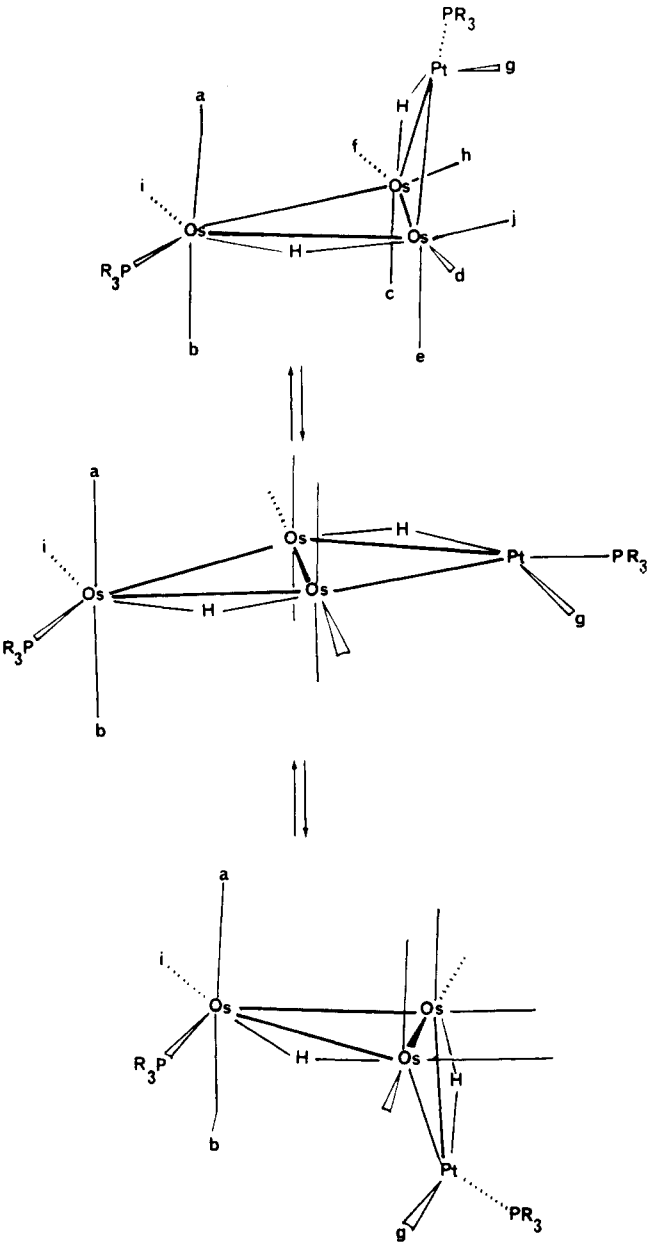

Experimental Section

General experimental techniques were as previously reported.[12] ^1H and ^{31}P NMR spectra were obtained on a Varian XL100 or a Bruker WP 200SY spectrometer. ^{13}C spectra at 50.3 and 90.56 MHz were recorded on a Bruker WP 200SY or WH 360, spectrometer, respectively, using samples enriched to at least 9%. Chemical shifts were referenced to internal solvent signals for ^{13}C and ^1H spectra and are reported relative to Me_4Si. ^{31}P spectra are referenced to external 85% H_3PO_4. For ^{13}C spectra $Cr(acac)_3$ was used as a shiftless relaxation agent. Dynamic NMR spectra were simulated by using a version of DNMR3[62] which was locally adapted to include exchanging ^{196}Pt satellites. Temperatures were calibrated by using the method of van Geet[63] and are considered accurate to ±2 K. Thermodynamic parameters were determined from the rate data by using standard methods.[64] To achieve high selectivity in the DANTE experiments, we used a sequence of ca. 50 on-resonance pulses of 0.6 s duration, spaced by 1 ms. This resulted in less than complete inversion of signals. A standard NOESY pulse sequence was used for the 2D exchange correlation study with the mixing time of 0.15 s varied randomly by ±15% to reduce correlations due to scalar couplings. A total of 256 1D spectra along the t_1 dimension were collected. The frequency domain matrices were symmetrized along the $F_1 = F_2$ diagonal.

Solutions of PCy_3 were prepared from the CS_2 adduct (Strem Chemicals) by refluxing in ethanol under a dinitrogen atmosphere. $Os_3Pt(\mu\text{-}H)_2(CO)_{10}(PCy_3)$ was prepared by the previously reported method.[1]

Preparation of ^{13}CO-Enriched $Os_3Pt(\mu\text{-}H)_2(CO)_{10}(PCy_3)$ (1). A sample of **1** (0.5 g) was dissolved in CH_2Cl_2 (20 mL), and 1-mL portions of ^{13}CO (99%, Cambrian Gases) were added via a mercury manometer system until the dark green color of **1** gave way to the yellow-brown color of the adduct $Os_3Pt(\mu\text{-}H)_2(CO)_{10}(^{13}CO)(PCy_3)$. Petroleum ether (bp 40–60 °C) (50 mL) was added and the solution refluxed under dinitrogen purge for 3 h to decarbonylate the complex. The resulting dark green solution was concentrated to ca. 20 mL and stored at −30 °C for 12 h affording black crystals of $Os_3Pt(\mu\text{-}H)_2(^*CO)_{10}(PCy_3)$ (0.34 g). The statistical level of enrichment in each CO site is ca. 9%.

Preparation of $[Os_3Pt(\mu\text{-}H)_3(CO)_{10}(PCy_3)]^+BF_4^-$ (2). Complex **1** (0.20 g, 0.15 mmol) was dissolved in CH_2Cl_2 (20 mL) and $HBF_4\text{-}Et_2O$ (0.1 mL) added. Careful addition of diethyl ether

(61) Churchill, M. R.; Hollander, F. J. *Inorg. Chem.* **1977**, *99*, 2493.
(62) Kleier, D. A.; Binsch, G. *QCPE* **1970**, *11*, 165.
(63) van Geet, A. L. *Anal. Chem.* **1970**, *42*, 679.
(64) Sandström, J. *Dynamic NMR Spectroscopy*; Academic: New York, 1982.

Table VII. Experimental Data for Crystallographic Study

formula	$C_{28}H_{36}BF_4O_{10}Os_3PPt$
M_r	1416.1
space group	Pn (No. 7, C_s^2)
cryst system	monoclinic
a/Å	9.925 (2)
b/Å	11.747 (3)
c/Å	16.186 (4)
β/deg	89.75 (2)
V/Å^3	1887.1 (8)
Z	2
D_{calcd}/g cm^{-3}	2.49
$F(000)$	1292
μ(Mo Kα)/cm^{-1}	139.3
T/K	298
scan mode	$\theta/2\theta$
θ range/deg	$2 < \theta < 30$
cryst size/mm	0.3 × 0.3 × 0.1
range of trans coeff corr	0.69–1.37
no. of data collected	5783
no. of unique data	5782
std reflctns	$\bar{3}5\bar{4}$, $\bar{4}35$
observability criterion n ($I > n\sigma(I)$)	3
no. of data in refinement	4087
no. of refined parameters	269/251
final R	0.032
R_w	0.034
largest remaining feature in elec. density map, e Å^{-3}	+1.42 (max), −1.62 (min)
shift/esd in last cycle	0.23 (max), 0.039 (av)

in 1-mL aliquots until the mother liquor is almost colorless affords dark green crystals of **2** (0.20 g, 0.14 mmol, 93% yield): IR (CH_2Cl_2, ν_{max}(CO)) 2124 (m), 2096 (vs), 2084 (vs), 2068 (s), 2046 (m), 2026 (s), 2004 (w) cm^{-1}; for NMR parameters see Table IV. Anal. Calcd for $C_{28}H_{36}BF_4O_{10}Os_3PPt$: C, 23.75; H, 2.56; P, 2.19. Found: C, 23.73; H, 2.12; P, 2.49. A ^{13}C-enriched sample of **2** was prepared in the above manner by using enriched samples of **1**.

Preparation of ^{13}CO-Enriched $Os_3Pt(\mu\text{-}H)_2(CO)_{11}(PCy_3)$ (3). A previously enriched sample of **1** was treated with 99% ^{13}CO until the green color had been discharged. The solution was cooled to −40 °C, purged with dinitrogen to remove excess ^{13}CO, and used directly for NMR studies. The statistical level of enrichment at each CO site is ca 18%.

Preparation of ^{13}CO-Enriched $Os_3Pt(\mu\text{-}H)_2(CO)_{10}(PCy_3)_2$ (4). In an analogous fashion to the previously reported method for the PPh_3 complex,[6] an enriched sample of **1** (0.3 g, 0.22 mmol) in CH_2Cl_2 (20 mL) was treated with a 1 molar equiv of PCy_3 solution in hexane. The brown-yellow solution was reduced in volume and chromatographed on a Florosil column by using hexane/CH_2Cl_2 (5:1) as an eluant. The bright yellow band was collected and evaporated in vacuo and the resulting oily residue used for the NMR studies.

Crystal Structure Determination. Details of data collection procedures and structure refinement are given in Table VII. Data were collected at ambient temperature on an Enraf-Nonius CAD4F automated diffractometer, with graphite-monochromated X-radiation (λ = 0.710 69 Å). Unit-cell parameters were determined by refinement of the setting angles ($\theta \geq 12°$) of 25 reflections. Standards were measured every 2 h during data collection, and no significant decay was observed. Lorentz/polarization and absorption (DIFABS[65]) corrections were applied. Systematic absences ($h0l$, $h + l = 2n + 1$) and Laue symmetry indicated the monoclinic space groups $P2/n$ or Pn. Analysis was initiated in the noncentrosymmetric Pn (nonstandard setting of Pc) on the basis of E statistics and density considerations and was confirmed by successful full-matrix refinement. The structure was solved by direct methods (MITHRIL[66]) and subsequent electron density difference syntheses. All non-hydrogen atoms were allowed anisotropic thermal motion. Hydrogen atoms were included at calculated positions (C–H = 1.073 Å for cyclohexyl groups, for hydridic protons (HYDEX[25]) Os–H and Pt–H = 1.85 Å) and were held fixed during refinement with fixed isotropic (0.05 Å^2) thermal parameters. Refinement was by full-matrix least squares. Due to matrix size limitations the parameter list was divided into two sections and each refined separately. The function minimized was $w(|F_o| - |F_c|)^2$ with the weighting function $w = [\sigma^2(F_o)]^{-1}$ used and judged satisfactory. $\sigma(F_o)$ was estimated from counting statistics. Neutral atom scattering factors were taken from ref 67 with corrections applied for anomalous dispersion. All calculations were carried out on a Gould-SEL 32/27 mini computer using the GX suite of programs.[68]

Acknowledgment. We wish to thank Johnson-Matthey for a generous loan of Pt salts, the SERC for a research studentship (to P.E.) and time on the high-field NMR service at Edinburgh, and D. Reed for running the 90.56-MHz ^{13}C NMR spectra.

Registry No. 1, 68091-56-5; 2, 112320-18-0; 3, 77700-90-4; 4, 112320-16-8.

Supplementary Material Available: Tables of anisotropic thermal parameters and calculated hydrogen atom positional parameters and complete listings of bond lengths and angles (5 pages); a listing of calculated and observed structure factors (23 pages). Ordering information is given on any current masthead page.

(65) Walker, N.; Stuart, D. *Acta Crystallogr., Sect. A: Found. Crystallogr.* **1983**, A*39*, 158.
(66) Gilmore, C. J. *J. Appl. Cryst.* **1984**, *17*, 42.
(67) *International Tables for X-Ray Crystallography*; Kynoch: Birmingham, 1974; Vol. 4.
(68) Mallinson, P. R.; Muir, K. W. *J. Appl. Cryst.* **1985**, *18*, 51.
(69) Farrugia, L. J. *Acta Crystallogr. Sect. C: Cryst. Struct. Commun.*, in press.